Physica B 668 (2023) 415225

Contents lists available at ScienceDirect

Physica B: Condensed Matter

journal homepage: www.elsevier.com/locate/physb

Evidence of Chlorotellurate(IV) – Hydroxochlorotellurate(IV) species equilibrium upon dissolution of tellurite glasses in aqueous hydrochloric acid: A Raman spectroscopic study

N.K. Nasikas [a,**], P. Siafarika [b], S. Tsigoias [b], C. Kouderis [b], S. Boghosian [c], A. G. Kalampounias [b,d,*]

[a] Division of Mathematics and Engineering Sciences, Department of Military Studies, Hellenic Army Academy, Vari, Attica, Greece
[b] Department of Chemistry, University of Ioannina, Ioannina, Greece
[c] Department of Chemical Engineering, University of Patras, Patras, Greece
[d] University Research Center of Ioannina (URCI), Institute of Materials Science and Computing, Ioannina, Greece

ARTICLE INFO

Keywords:
Tellurite glasses
Chlorotellurates
Hydroxochlorotellurates
Raman spectroscopy
Solutions
Short-range order

ABSTRACT

Raman spectroscopy has been used to elucidate the structure of tellurium (IV) oxide and its binary mixtures with thallium oxide both in the glassy state and in aqueous hydrochloric acid solutions. The addition of Tl_2O in pure TeO_2 glass results in the progressive transformation of TeO_4 trigonal bipyramid (tbp) to TeO_3 trigonal pyramid (tp) units in agreement with the literature findings. Thallium oxide acting as a modifier for the tellurite network, reduces the functionality of the initial unit and lowers the continuous network rigidity. The spectral changes upon dissolution of the $0.2Tl_2O$-$0.8TeO_2$ glass in aqueous hydrochloric acid solution have also been measured revealing that the main structural units of the glass structure did not survive in a solution state and the connectivity of the glass network has completely collapsed. The systematics and the concentration dependence of the spectra acquired from different solutions indicate the presence of several chlorotellurate(IV) and hydroxochlorotellurate(IV) ionic species. The spectroscopic data are interpreted in such a way in order to indicate a dynamic equilibrium between the $TeCl_6^{2-}$ anion and the $TeCl_4(OH)^-$ species. A combined analysis of the polarized and depolarized scattered intensity is presented here which aimed at elucidating the presence of additional species including the $TeCl_4(OH)_2^{2-}$ and $TeCl_3(OH)$ species, respectively. The proposed model is discussed in the framework of the current phenomenological status of the field.

All authors have read and agreed to the published version of the manuscript.

1. Introduction

Pure tellurium oxide and tellurium oxide-based glasses have been the subject of intense research mainly due to their interesting electrical and optical properties. Leading highlights include extended infrared transmittance [1], high optical indices both linear and non-linear [2], low melting points, and relatively good chemical resistance. Advantages of tellurite glasses include reasonably wide transmission range, from visible to mid-IR (~400 nm–6 μm), good glass stability, strength and corrosion resistance, relatively low phonon energy for an oxide glass (≈800 cm^{-1}) for amplification applications, high refractive index (≈2) for non-linear applications, high third-order optical non-linearity (1.9572×10^{-20} m^2/V^2) with several orders of magnitude larger than that of conventional silicate and borate glasses, and ease of fabrication due to presence of the modifier oxide which reduces significantly the melting point of TeO_2 (~733 °C) [1,2]. The origin of these properties is directly related with the local order and coordination around tellurium atoms.

In the linear optical domain, photons interact with the glass structure leading to various optical effects, including dispersion, refraction, reflection, absorption, diffraction, and scattering. The linear refractive

* Corresponding author. Department of Chemistry, University of Ioannina, GR-45110, Ioannina, Greece.
** Corresponding author. Division of Mathematics and Engineering Sciences, Department of Military Studies, Hellenic Army Academy, GR 16673, Vari, Attica, Greece.
E-mail addresses: nasikas@sse.gr (N.K. Nasikas), akalamp@uoi.gr (A.G. Kalampounias).

https://doi.org/10.1016/j.physb.2023.415225
Received 11 July 2023; Received in revised form 2 August 2023; Accepted 16 August 2023
Available online 17 August 2023
0921-4526/© 2023 Elsevier B.V. All rights reserved.

index of a material, n, describes how light propagates through it, and the index defines how much light is bent, or refracted when it across the material. Nevertheless, these properties may become non-linear if the intensity is high enough to modify the glass optical properties, resulting in the creation of new beam lights of different wavelengths. A non-linear optical behavior is a deviation from the linear interaction between a material's polarization response and the electric component of an applied electromagnetic field. This phenomenon involves various optical exchanges such as frequency doubling, conversion, data transformation, etc. Because the magnetic component of light can be ignored in a glass since photons and magnetic fields usually do not interact, the electric component (E) becomes the main field that interacts with the medium. The polarization (P) induced by this interaction produces nonlinear responses that can be explained due to the distortion/deflection of the electronic structure of any atom or molecule (deformation of the electron cloud) due to the application of the electric field, thus producing a resulting dipole moment (vector that separates the positive and negative charges). Once an external E field is applied to the material the positive charges tend to move in the opposite direction of the electrons. This interaction causes a charge separation that gives rise to microscopic dipole moments within the material. Under the influence of an electric field, these dipoles oscillate at the same frequency (ω) of the incident light. The sum of all the microscopic dipoles of the medium oscillating with time gives rise to material polarization. The interest in non-linear optical properties of glass appears with the development of high-power lasers and the growth of the optical information transmission in the telecom sector. For instance, the Kerr effect (third order nonlinearity), at the origin for a change in the refractive index with the laser intensity, is responsible for a spectacular self-focusing phenomenon due to the formation of a photo-induced lens directly linked to the intensity-spatial profile of the beam. The structure of tellurite systems has been explored by a variety of techniques including X-ray diffraction, Raman spectroscopy, neutron diffraction, etc. [3–6].

The chemical nature and the amount of the glassy network modifier in the binary tellurite glasses strongly affect the coordination geometry of the *Te* atoms. Addition of an alkali oxide in the pure TeO_2 matrix, alters the coordination of *Te* atoms from four-fold to three-fold with the transformation of the trigonal bipyramid (tbp) TeO_4 units with two axial and two equatorial oxygen atoms to a trigonal pyramid (tp) TeO_3 groups via intermediate TeO_{3+1} polyhedra [7,8]. With increasing modifier content, the TeO_{3+1} polyhedra are formed from the TeO_4 tbp groups through shortening of one of the axial bonds with a parallel elongation of one equatorial bond. In TeO_4 tbp units, the third equatorial site of the sp^3d hybrid orbital is occupied by an electronic pair, which is of key importance in the structural and non-linear properties of the mixed tellurite glasses. Thallium oxide (Tl_2O) has attracted a great attention as a modifier oxide since its addition, contrary to other modifier oxides leads to maintain the amplitude of the high optical non-linearity of the TeO_2-based materials, despite the structural depolymerization of the glasses evidenced by Raman spectroscopy.

Incorporation of a modifier oxide into TeO_2 amorphous phase leads to a reduction in the coordination number of Te cation by the transformation of initially present TeO_4 disphenoids into TeO_3 trigonal pyramidal units. The decrease in the coordination number generally leads to a decrease of the non-linear optical response of the material, the opposite trend is observed in the case of Tl_2O modifier. Thus, in order to prepare a new class of TeO_2-based glasses with all the attractive properties of the mixed oxides with the high optical non-linearity of pure TeO_2, the thallium oxide should be used as the second component-modifier oxide.

Nevertheless, much less attention has been paid to the dissolution of these glasses in acidic solutions in order to evaluate the sustainability of these building groups in solution state and the disposability assessment of the corresponding glasses. It has been reported that sodium tellurite, an inorganic tellurium compound with formula Na_2TeO_3, was found to be easily soluble in aqueous solutions, which is important when considering glass durability [9]. In aqueous hydrochloric acid solutions, tellurium (IV) atoms form a series of complexes. The composition of these complexes depends strongly on the preparation and processing of the solutions [10]. Certain of these complexes have been inadequately characterized probably due to the inherent complex equilibria, which involves the transition of tellurium oxyanions into chloride complexes [10 and references therein].

In this study, the xTl_2O-$(1-x)TeO_2$ glasses were prepared and their structure was investigated by means of Raman spectroscopy. The results agreed with the existing information on these glasses. Furthermore, the tellurium based $0.2Tl_2O$-$0.8TeO_2$ glass was dissolved in aqueous hydrochloric acid solution at various concentrations, in order to elucidate the *Te*(IV) species present in these solution and access the structural parameters involving *Te* coordination by oxygen or chlorine atoms.

2. Experimental

2.1. Materials

Tellurium (IV) oxide and thallium carbonate of reagent grade were purchased from *Alfa Aesar* (purity 99.99%) and *Merck* (purity 99%), respectively. TeO_2 in crystalline form was used as received, while Tl_2O was dried for a few hours. The required amounts of thallium carbonate and tellurium oxide were mixed and melted in a *Pt* crucible for several minutes in a temperature range between 700 and 800 °C. All glasses were formed by dipping the bottom of the crucible into ice-cold water. More details about the preparation of samples can be found elsewhere [11]. The homogeneous and amorphous nature of the xTl_2O-$(1-x)TeO_2$ glasses was checked by X-ray diffraction (XRD). XRD patterns were obtained with the aid of a Philips X'Pert MPD diffractometer using Cu Kα radiation in $\theta-2\theta$ scans and grazing incidence 2θ scans ($\theta = 1°$). The XRD patterns of the glasses are presented in Fig. S1 of the Supplementary Material. This figure reveals that all XRD traces exhibit featureless structure, being similar to each other for the various x, and correspond to completely amorphous materials.

For the preparation of the solutions, the desired amount of $0.2Tl_2O$-$0.8TeO_2$ glass was dissolved in 3 ml aqueous *HCl* solution with a concentration of 12 M (37%) applying continuous stirring under ambient conditions. The stock *HCl* solution of *ACS* reagent grade was received from *Sigma-Aldrich*. Homogeneous pale yellowish solutions were prepared following the above. All spectroscopic measurements were performed in fresh solutions that had just been prepared. The molar concentrations of the prepared aqueous *HCl* solutions, as well as the corresponding mass of the glass dissolved in solution are presented in Table 1.

2.2. Vibrational spectroscopy

All polarized (Vertical – Vertical: *VV*) and depolarized (Vertical – Horizontal: *VH*) Raman spectra were excited by the 532.0 nm linearly polarized laser line and recorded in a 180° scattering geometry by means of the *LabRAM Soleil* Raman spectrometer (*Horiba*, *Jobin Yvon*). After the

Table 1
Molar concentrations of the prepared aqueous *HCl* solutions.

Solution #	Mass (g of glass dissolved in solution)	Molar concentration (mM)
1	0.0105	25.7
2	0.0125	30.6
3	0.0200	49.0
4	0.0277	67.8
5	0.0477	116.8
6	0.0695	170.2
7	0.0837	205.0
8	0.1943	476.0
9	0.2860	700.6
10	0.3740	916.1

monochromator's gratings, Raman photons were detected by a two-dimensional CCD detector that is thermoelectrically cooled. The rejection of the elastic Rayleigh scattering was achieved by means of a notch filter appropriate for the 532.0 nm wavelength. To reduce sample irradiance, the power level on the sample was fixed by employing specific power density filters, thereby ensuring that there is no heating of the sample taking place. The spectral resolution of all measurements was set at 1.5 cm^{-1}. A CCl_4 reference sample sealed in fused silica tube was utilized in order to check the depolarization ratio accuracy of the Raman polarization measurements and correct for possible drifts of the monochromator. Quantitative Raman intensity measurements were possible with an experimental error lower than ±2%. More details about the experimental setup and the procedures for acquiring polarization dependent Raman measurements in the liquid and glassy state can be found elsewhere [12–16].

The Fourier-transform infrared (FTIR) spectroscopy has been employed to identify the species present in the structure of the glasses. All spectra were measured at room temperature using an Alpha spectrometer (Bruker) using a DTGS detector. The spectra of solids were measured using the standard KBr pellet method operating in transmittance mode with a spectral resolution of 2 cm^{-1}. The spectra correspond to the average of 32 individual scans.

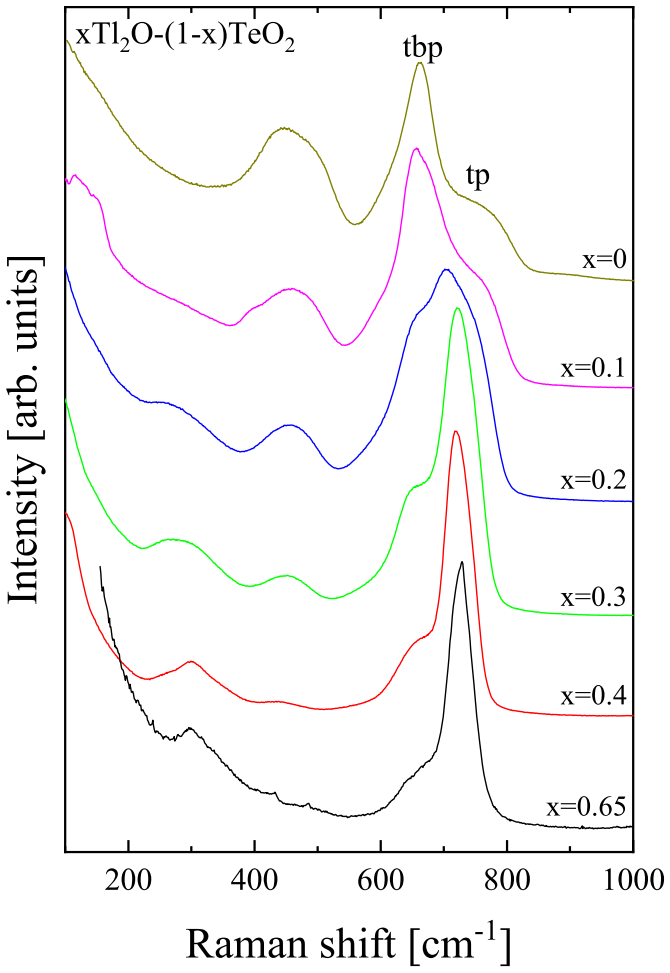

Fig. 1. Representative Stokes-side polarized (*VV*) Raman spectra of xTl_2O-$(1-x)TeO_2$ glasses at various Tl_2O mole fractions under ambient conditions. Spectral conditions: spectral slit width = 1.5 cm^{-1}, excitation line = 532.0 nm.

3. Results and discussion

3.1. The structure of Tl_2O–TeO_2 glasses

Fig. 1 shows the polarized (*VV*) Raman spectra of the xTl_2O-$(1-x)TeO_2$ glasses recorded under ambient conditions. The spectra shown in Fig. 1 are similar to those reported previously in the literature [17–19]. The structure of pure TeO_2 glass is dominated by TeO_4 trigonal bipyramid units (tbp) with the one equatorial site of the sp^3d hybrid orbitals to be occupied by a lone pair of electrons. The axial and other two equatorial sites are occupied by oxygen atoms. The addition of Tl_2O significantly alters the structure of pure TeO_2 glass thus acting as a modifier for the tellurite network [19,20]. The main modification is the structural change from TeO_4 tbp to TeO_3 trigonal pyramid (tp). The TeO_3 units have one of the Te sp^3 hybrid orbitals occupied by a lone pair of electrons. The peaks in the 600-680 cm^{-1} region are assigned to the TeO_4 tbp units, while the most intense Raman bands at 720-725 cm^{-1} are attributed to isolated TeO_3 tp anions.

The bands that are resolved in the 400-600 cm^{-1} spectral region are assigned to the bending modes of *Te–O–Te* or *O–Te–O* bridges. The TeO_3 tp units possess terminal bonds including the $Te-O^-$ and $Te=O$ bonds [19,20]. Considering that the basic coordination of TeO_4 tbp polyhedra are the $TeO_{3/2}O^-$ and the $TeO_{1/2}O^-(=O)$, then the gradual transformation from the tbp's to tp's could be performed through the following reaction schemes [7 and references therein]:

$$TeO_{4/2} \rightleftarrows TeO_{2/2}(=O) \quad (1)$$

$$TeO_{3/2}O^- \rightleftarrows TeO_{1/2}O^-(=O) \quad (2)$$

The structural units present in the xTl_2O-$(1-x)TeO_2$ binary tellurite glasses are shown schematically in Fig. 2.

It was proposed that if the cation strength of the added atom is lower than that of *Te*, then the oxygen atoms of the added oxide attack the coordination spheres of *Te* causing an increase of the number of $Te-O$ terminal bonds with a parallel transformation of TeO_4 to TeO_3 units [21]. On the other hand, if the cation strength of the added atom is similar to that of *Te*, the TeO_3 tp units would not be formed and the initial structure will not be destroyed. In this case, the Raman spectrum will be dominated by the double band centered near ~650 cm^{-1} in close resemblance with the spectrum of pure TeO_2 glass [21,22]. In the Raman spectra of the binary xTl_2O-$(1-x)TeO_2$ glassy system presented in Fig. 1 for x up to 0.65, the bands attributed to TeO_4 tbp and TeO_3 tp structural units coexist, demonstrating the simultaneous presence of framework-like structure interconnected through *Te–O–Te* or *O–Te–O* linkages and of the *ortho*-tellurite constitution which involves the TeO_3 tp units [19]. The progressive transformation of TeO_4 tbp to TeO_3 tp units reduces the functionality of the initial unit and thus, lowers the continuous network rigidity in agreement with previous studies [19–22]. Analogous gradual transformation from the tbp's to tp's is also observed in the FTIR spectra that are presented in Fig. S2 of the Supplementary Material. The infrared absorbance spectra for glasses up to x = 0.4 mol fraction reveal broad bands characteristic of completely amorphous materials. The terminal composition with x = 0.5 mol fraction corresponds to a partially crystalline glassy phase. This crystalline phase is attributed to the orthotellurite Tl_2TeO_3, which consists of isolated TeO_3 trigonal pyramids separated by Tl cations. The bands at ~550-600 cm^{-1} are assigned to stretching vibrations of TeO_4 tbp. The bands observed at ~670-720 cm^{-1} are related to stretching vibrations of the TeO_3 tp species. Finally, the region at ~400-500 cm^{-1} corresponds to bending vibrational modes of Te–O–Te or O–Te–O linkages present in the tellurite glass network.

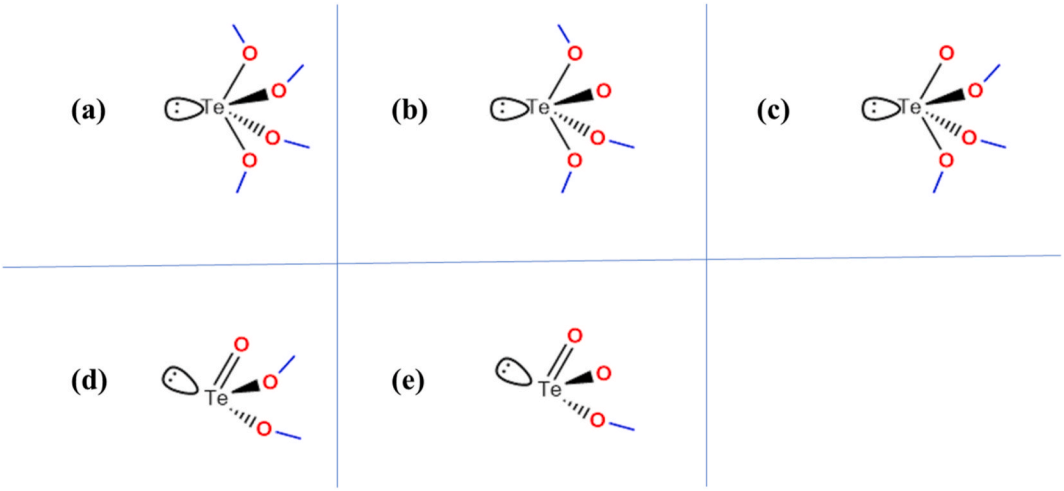

Fig. 2. The tellurite species present in the structure of binary tellurite glasses. (a) TeO_4 trigonal bipyramid unit; (b) $TeO_{3/2}O^-$ isomeric trigonal bipyramid unit with one non-bridging oxygen atom in equatorial site; (c) $TeO_{3/2}O^-$ isomeric trigonal bipyramid unit with one non-bridging oxygen atom in axial site; (d) TeO_3 trigonal pyramid unit; and (e) $TeO_{1/2}O^-(=O)$ trigonal pyramid unit with one charged and one neutral non-bridging oxygen atom, respectively. The O^- denotes the non-bridging oxygen atoms.

3.2. Study of thallium tellurite glasses dissolved in hydrochloric acid solutions

As reviewed in the previous section, the structure of thallium tellurite glasses is characterized by the presence of TeO_4 tbp and TeO_3 tp building units and their relative population depends on the Tl_2O modifier content in the binary glasses. The purpose of this work is to examine based on the Raman spectra if these species survive upon dissolution of the modified tellurite glass in aqueous hydrochloric acid. Fig. 3 shows the polarized (*VV*) Raman spectra for all solution concentrations of the $0.2Tl_2O$-$0.8TeO_2$ glass dissolved in 12 M aqueous *HCl* prepared in this work. The spectrum of water is also presented in the bottom for direct comparison. The intensity of the low-frequency bands gradually increases when increasing the concentration of the solutions.

The Raman scattering spectrum of pure water is dominated by a shoulder band located at ~3250 cm^{-1}, which corresponds to the asymmetric *–OH* stretch, the most intense band near ~3410 cm^{-1} that corresponds to the symmetric *–OH* stretch and a smaller shoulder band

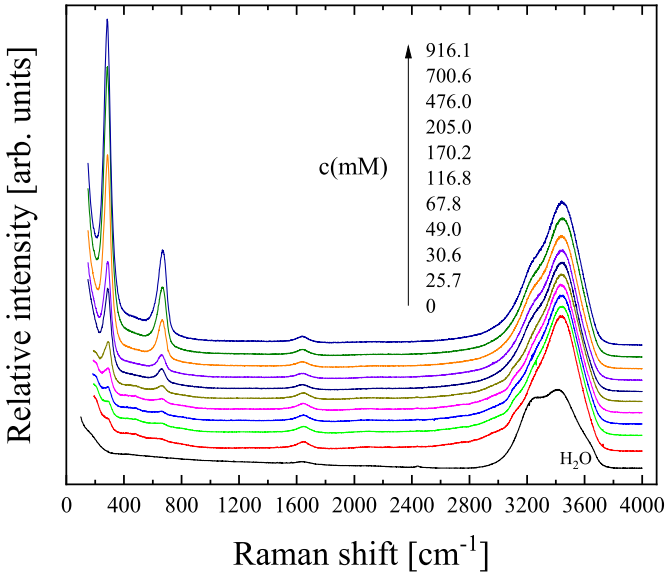

Fig. 3. Polarized (*VV*) Stokes-side Raman spectra of $0.2Tl_2O$-$0.8TeO_2$ glass dissolved in aqueous *HCl* 12 M solution.

at ~3630 cm^{-1} which is assigned to the *–OH* stretch of a water molecule which is only partially involved in hydrogen bonding. A simple approach of the overall water structure is a hydrogen-bonded tetrahedrally coordinated network comparable to that of ice. In this structural entity, a few interstitial cavities are filled by water molecules [23–25]. This local long-range tetrahedral structure of water has a short lifetime of the order of less than 0.1 ps, while it is changing constantly throughout breaking and forming of hydrogen bonds. A more complicated view of the water structure is that it is a mixture of different types of regions varying from free water molecules to randomly bonded molecules and ordered regions [26]. The addition of *HCl* and tellurite glass affects the interplay between the various *–OH* stretching modes in the high frequency part of the spectra presented in Fig. 3. The stability of water clathrates and the overall hydrogen-bonding network is strongly influenced by the presence of salt species. In the medium frequency range near 1600–1650 cm^{-1}, a very weak peak is observed, which is also strongly dependent on the associativity of water [27]. Thus, in order to examine in detail, the spectral features that are attributed to tellurium-based species, we will focus our attention on the frequency range below 1000 cm^{-1}.

Fig. 4 illustrates representative polarized (*VV*) Raman spectra of the solutions obtained upon dissolution of the $0.2Tl_2O$-$0.8TeO_2$ glass in aqueous hydrochloric acid solution. The spectra of pure TeO_2 and $0.65Tl_2O$-$0.35TeO_2$ glasses are also shown for comparison. The results reveal that the most intense Raman bands of the $0.65Tl_2O$-$0.35TeO_2$ glass at 720-725 cm^{-1} attributed to TeO_3 trigonal pyramid are absent in the spectra of solutions implying that these groups are not surviving in solutions. The bands resolved in the 400-600 cm^{-1} spectral region of pure TeO_2 glass that are assigned to the bending modes of *Te–O–Te* or *O–Te–O* bridges are also absent in the spectra of solutions indicating the collapsing of the glass network upon dissolution. The only common spectral feature between the spectra of glasses and solutions is the presence of the broad band in the 600-680 cm^{-1} region that are assigned to the TeO_4 tbp units for the tellurite glasses. In solutions, this band is probably due to species containing $Te-O$ bonds. In the low-frequency part, the spectra of solutions are dominated by a strong asymmetric spectral feature near ~300 cm^{-1}, which rapidly gains in intensity with increasing solution concentration.

Let us now focus on the polarized (*VV*) Raman spectra of solutions at frequencies below 800 cm^{-1} that are presented in Fig. 5 (a). The spectrum of pure water is also included for comparison. The most intense bands are observed near ~284 and ~669 cm^{-1} that are assigned to

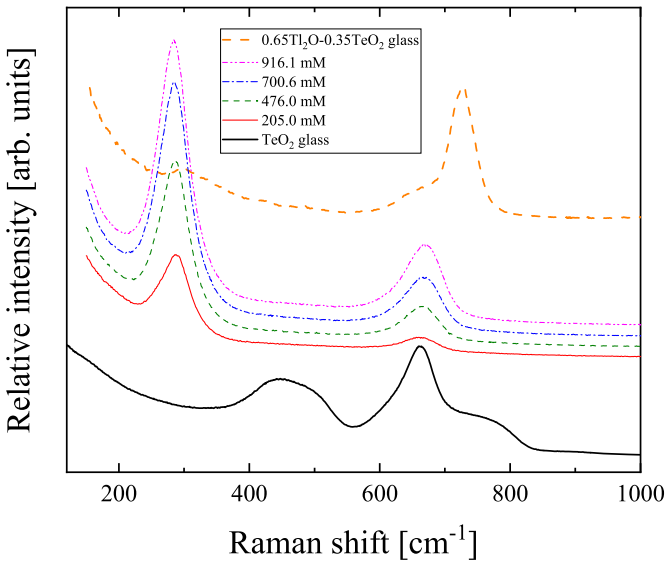

Fig. 4. Representative polarized (*VV*) Raman spectra of *0.2Tl$_2$O-0.8TeO$_2$* glass dissolved in 3 ml aqueous *HCl* 12 M solution. The spectra of pure *TeO$_2$* (bottom) and *0.65Tl$_2$O-0.35TeO$_2$* (top) glasses are shown for comparison.

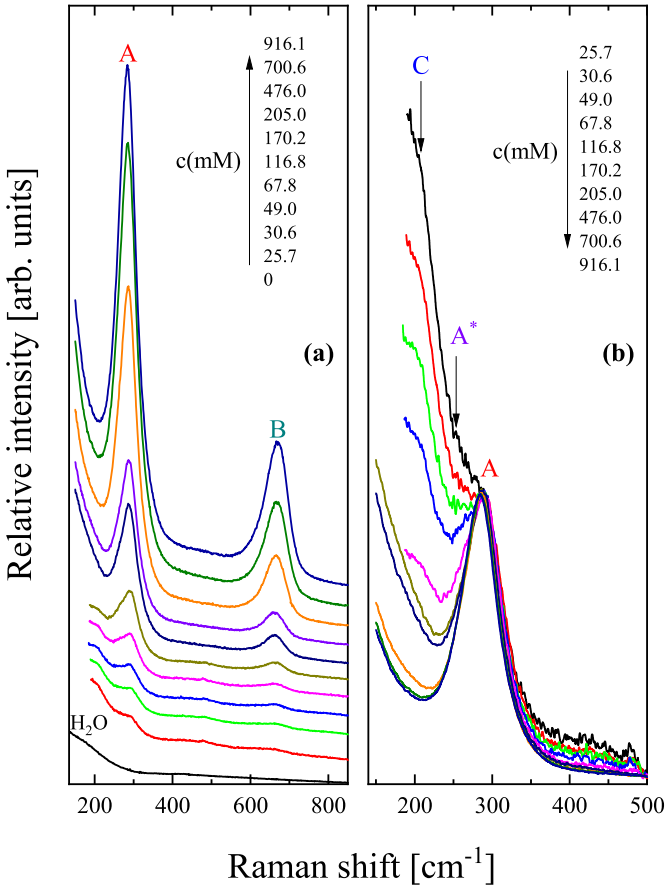

Fig. 5. (a) Low-frequency polarized (*VV*) Raman spectra of *0.2Tl$_2$O-0.8TeO$_2$* glass dissolved in 3 ml aqueous *HCl* 12 M solution. The spectrum of pure water is also included for comparison. **(b)** Raman spectra for all concentrations studied in the low-frequency region. All spectra have been normalized with respect to band A to estimate the spectral intensity changes induced by concentration.

octahedral $TeCl_6^{2-}$ and trigonal bipyramidic $TeCl_4(OH)^-$ ionic species with an apical oxygen atom, respectively [28–30]. The chlorotellurate $TeCl_6^{2-}$ anion is in dynamic equilibrium with the hydroxochlorotellurate (IV) $TeCl_4(OH)^-$ species according to:

$$TeCl_6^{2-} + H_2O \rightleftarrows TeCl_4(OH)^- + Cl^- + HCl \quad (3)$$

To resolve the spectral characteristic observed below 300 cm^{-1}, we have chosen to normalize all spectra to the intensity of band *A* and the results are shown in Fig. 5 (b). This way, we can effectively estimate the spectral intensity changes induced by concentration. It seems that band *A* shifts to lower frequencies with increasing concentration. Two additional peaks are resolved except *A* band denoted as *A** and *C* that are located at ~254 and ~208 cm^{-1}, respectively. Band *C* is assigned to another halide species, the $TeCl_x$, which is favored at low concentrations as evidenced from Fig. 5 (a). With increasing solution concentration, the Raman intensity of *A** and *C* bands decreases relative to the intensity of band *A*. The fact that the intensity of *C* reduces compared to the intensity of band *A* with concentration implies that these bands originate from completely different species.

In Fig. 6, we present the relative Raman intensities in arbitrary units of the *A*, *B*, *A** and *C* bands as a function of solution concentration. The results reveal that the behavior of *A** and *B* bands is comparable and probably band *A** may be attributed to the *Te–Cl* stretching mode presence of a possible trigonal bipyramidic $TeCl_3(OH)$ species. The latter species could have a trigonal bipyramid structure with two chlorine atoms in equatorial and one in axial site, respectively. In addition, the Raman intensity of band *A* exhibits the greatest increase with concentration indicating that chlorotellurate $TeCl_6^{2-}$ octahedral species are favored at higher concentrations. The chlorotellurate(IV) and hydroxochlorotellurate(IV) species participating in the structure of the aqueous hydrochloric acid solutions are illustrated schematically in Fig. 7.

If we assume that the integrated intensities of bands *A*, *B*, *A** and *C* are proportional to the populations of the corresponding species involved, then Fig. 6 is indicative of the population variation of the respective species as a function of concentration. Due to lack of any relevant information, we implicitly assumed here that the Raman cross-section of the vibrational modes of the *Te* species are comparable.

The analysis of the Raman experimental data in terms of polarization geometry is usually overlooked, even though this way a great amount of information can be retrieved. Fig. 8 depicts the polarized (*VV*) and depolarized (*VH*) Raman spectra of a representative solution with

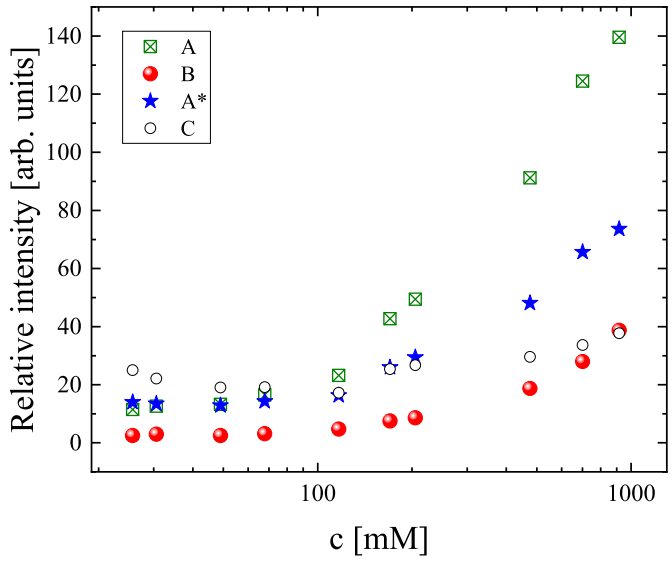

Fig. 6. Relative Raman intensity variation with concentration. The intensities correspond to *A*, *B*, *A** and *C* bands shown in Figs. 4 and 5.

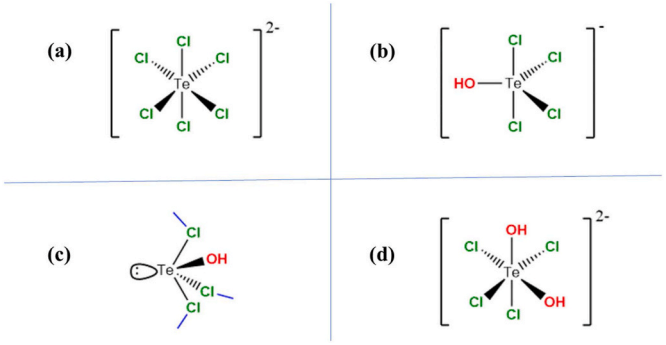

Fig. 7. The structural species present in the studied solutions: (a) the octahedral $TeCl_6^{2-}$ anion; (b) the trigonal bipyramidic $TeCl_4(OH)^-$ anion; (c) the trigonal bipyramidic $TeCl_3(OH)$ neutral species; and (d) the octahedral $TeCl_4(OH)_2^{2-}$ ionic species.

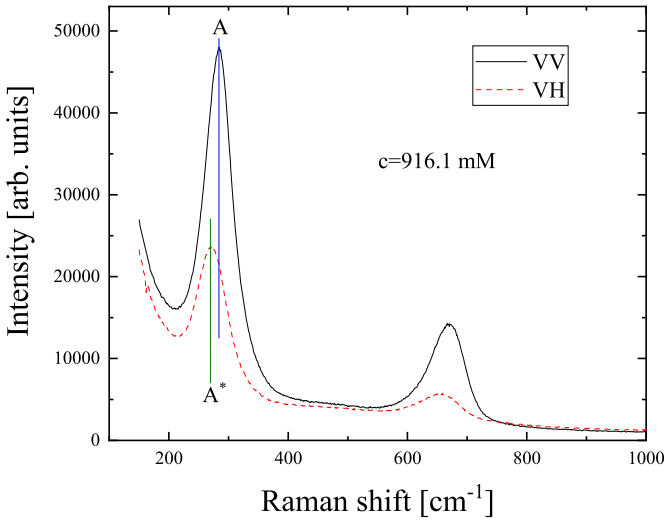

Fig. 8. Polarized (*VV*) and depolarized (*VH*) Raman spectra of a representative solution with concentration c = 916.1 mM in the frequency range below 1000 cm^{-1}.

concentration equal to 916.1 mM. The broad band at ~669 cm^{-1} that corresponds to hydroxochlorotellurate(IV) $TeCl_4(OH)^-$ ionic species appears highly polarized. The non-coincidence of the peak maximum in the *VV* and *VH* polarization implies the presence of additional species with more than one Te–O bond with a frequency in the 600-700 cm^{-1} stretching region, such as the $TeCl_4(OH)_2^{2-}$ ionic species. In the low-frequency part of the spectrum, the most intense and broad band observed near ~284 cm^{-1} is assigned to chlorotellurate $TeCl_6^{2-}$ species. The population of this species is negligible in solutions with hydrochloric acid concentration below 4.5 M [28]. Also, in the low-frequency region of the spectrum, the non-coincidence of the peak maximum in the *VV* and *VH* polarization implies the presence of two different bands with distinct polarization characteristics, namely the *A* and *A** bands attributed to $TeCl_6^{2-}$ and $TeCl_3(OH)$ species.

4. Conclusions

The following main conclusions may be drawn from the present study. The addition of Tl_2O significantly alters the structure of pure TeO_2 glass acting as modifier for the tellurite network in agreement with the literature findings. The progressive transformation of TeO_4 tbp to TeO_3 tp units reduces the functionality of the initial unit and lowers the continuous network rigidity. Upon dissolution of the $0.2Tl_2O$-$0.8TeO_2$ glass in aqueous hydrochloric acid solution, the main structural units of the glass structure do not survive in solution. Collapsing of the glass network is evidenced by the absence of modes due to *Te–O–Te/O–Te–O* linkages in the Raman spectra of solutions. The chlorotellurate $TeCl_6^{2-}$ anion, which is favored at higher concentrations, is in dynamic equilibrium with the hydroxochlorotellurate(IV) $TeCl_4(OH)^-$ species. The formation of $TeCl_3(OH)$ species is not excluded. The non-coincidence of the peak maximum in the *VV* and *VH* polarization reveals the presence of additional species with more than one Te–O bond with a frequency in the 600-700 cm^{-1} stretching region, such as the $TeCl_4(OH)_2^{2-}$ ionic species and the $TeCl_3(OH)$ species. Clearly, the above information reveals the complexity of analogous vitreous systems involving tellurite glasses and their dissolution behavior. Especially for defense related applications, where the decommission of various devices containing tellurite-based glass components, one needs to be very cautious when using dissolution methods in order to recycle or discharge them. This work opens up this field where limited work has been carried out so far and brings to the forefront the need for more systematic investigation.

Funding

This research received no external funding.

CRediT authorship contribution statement

N.K. Nasikas: Methodology, Investigation, Validation, Writing – review & editing. **P. Siafarika:** Investigation, Validation, Writing – review & editing. **S. Tsigoias:** Investigation, Validation, Writing – review & editing. **C. Kouderis:** Investigation, Validation, Writing – review & editing. **S. Boghosian:** Methodology, Investigation, Validation, Formal analysis, Data curation, Resources, Writing – review & editing. **A.G. Kalampounias:** Conceptualization, Methodology, Investigation, Validation, Formal analysis, Data curation, Resources, Writing – original draft, Writing – review & editing, Supervision, Project administration.

Declaration of competing interest

The authors declare that they have no known competing financial interests or personal relationships that could have appeared to influence the work reported in this paper.

Data availability

Data will be made available on request.

Acknowledgments

P. Siafarika acknowledges support by project “Dioni: Computing Infrastructure for Big-Data Processing and Analysis” (MIS No. 5047222) co-funded by European Union (ERDF) and Greece through Operational Program “Competitiveness, Entrepreneurship and Innovation”, NSRF 2014–2020.

Appendix A. Supplementary data

Supplementary data to this article can be found online at https://doi.org/10.1016/j.physb.2023.415225.

References

[1] M.J. Waber, J.D. Meyers, D.H. Blackburn, J. Appl. Phys. 52 (1981) 2944.
[2] K. Shioya, T. Kmatsu, H.G. Kim, R. Sato, K. Matusita, J. Non-Cryst. Solids 189 (1995) 16.
[3] G.W. Brady, J. Chem. Phys. 27 (1957) 300.
[4] A.G. Kalampounias, G. Tsilomelekis, S. Boghosian, J. Chem. Phys. 142 (2015), 154503.

[5] A.G. Kalampounias, N.K. Nasikas, G.N. Papatheodorou, J. Phys. Chem. Solid. 72 (2011) 1052.
[6] J.C. McLaughlin, S.L. Tagg, J.W. Zwanziger, J. Phys. Chem. B 105 (2001) 67.
[7] A.G. Kalampounias, S. Boghosian, Vib. Spectrosc. 59 (2012) 18.
[8] A.G. Kalampounias, G.N. Papatheodorou, S.N. Yannopoulos, J. Phys. Chem. Solid. 67 (2006) 725.
[9] E. Philippot, M. Maurin, J. Moret, Acta Crystallogr. B 35 (1979) 1337.
[10] J. Molue, M. Mahadaven, Inorg. Chem. 23 (1984) 268.
[11] A.G. Kalampounias, G.N. Papatheodorou, S.N. Yannopoulos, J. Phys. Chem. Solid. 68 (2007) 1029.
[12] A.G. Kalampounias, S.A. Kirillov, W. Steffen, S.N. Yannopoulos, J. Mol. Struct. (2003) 651–653, 475.
[13] A.G. Kalampounias, S.N. Yannopoulos, G.N. Papatheodorou, J. Chem. Phys. 124 (2006), 014504.
[14] A.G. Kalampounias, G. Tsilomelekis, S. Boghosian, Vib. Spectrosc. 65 (2013) 66.
[15] A.G. Kalampounias, G. Tsilomelekis, S. Boghosian, Spectrochim. Acta 135 (2015) 31.
[16] A.G. Kalampounias, G.N. Papatheodorou, J. Phys. Chem. Solid. 117 (2018) 70.
[17] T. Sekiya, N. Mochida, A. Ohtsuka, M. Tonokawa, J. Non-Cryst. Solids 144 (1992) 128–144.
[18] B. Jeansannetas, S. Blanchandin, P. Thomas, P. Marchet, J.C. Champarnaud-Mesjard, T. Merle-Me′jean, B. Frit, V. Nazabal, E. Fargin, G.L. Flem, M.O. Martin, B. Bousquet, L. Canioni, S.L. Boiteux, P. Segonds, L. Sarger, J. Solid State Chem. 146 (1999) 329.
[19] O. Noguera, T. Merle-Me′jean, A.P. Mirgorodsky, P. Thomas, J.C. Champarnaud-Mesjard, J. Phys. Chem. Solid. 65 (2004) 981.
[20] T. Sekiya, N. Mochida, A. Ohtsuka, J. Non-Cryst. Solids 168 (1994) 106.
[21] M. Soulis, A.P. Mirgorodsky, T. Merle-Me′jean, O. Masson, P. Thomas, M. Udovic, J. Non-Cryst. Solids 354 (2008) 143.
[22] O. Noguera, T. Merle-Me′jean, A.P. Mirgorodsky, M. Smirnov, P. Thomas, J.-C. Champarnaud-Mesjard, J. Non-Cryst. Solids 330 (2003) 50.
[23] O. Popovych, R.P.T. Tomkins, Nonaqueous Solution Chemistry, Wiley, New York, 1981.
[24] S. Burikov, T. Dolenko, S. Patsaeva, Y. Starokurov, V. Yuzhakov, Mol. Phys. 108 (2010) 2427.
[25] A. Laaksonen, P.G. Kusalik, I.M. Svishchev, J. Phys. Chem. A 101 (1997) 5910.
[26] C. Reichardt, Solvents and Solvent Effects in Organic Chemistry, second ed., VCH, Weinheim, 1988.
[27] J.H. Hibben, Chem. Rev. 13 (1933) 345.
[28] J.B. Milne, M. Mahadevan, Inorg. Chem. 23 (1984) 268.
[29] J.B. Milne, Can. J. Chem. 69 (1991) 987.
[30] I.M. Ivanov, S.V. Tkachev, S.N. Ivanova, J. Struct. Chem. 44 (2003) 146.